

*Prepared as a contribution to the conference proceedings of “Meteoroids 2004”, to be published in the journal “Earth, Moon, and Planets”.*

## **Preparing for Hyperseed MAC: an observing campaign to monitor the entry of the Genesis Sample Return Capsule**

PETER JENNISKENS,<sup>1,\*</sup> PAUL WERCINSKI,<sup>2</sup> JOE OLEJNICZAK,<sup>2</sup> GARY ALLEN,<sup>3</sup> PRASUN N. DESAI,<sup>4</sup> GEORGE RAICHE,<sup>2</sup> DEAN KONTINOS,<sup>2</sup> DOUG REVELLE,<sup>5</sup> JASON HATTON,<sup>6</sup> RICHARD L. BAKER,<sup>7</sup> RAY W. RUSSELL,<sup>7</sup> MIKE TAYLOR,<sup>8</sup> and FRANS RIETMEIJER<sup>9</sup>

<sup>1</sup>SETI Institute, 515 N. Whisman Rd., Mountain View, CA; <sup>2</sup>NASA Ames Research Center, Moffett Field, CA

<sup>3</sup>ELORET Institute, Sunnyvale, CA; <sup>4</sup>NASA Langley Research Center, Hampton, VA

<sup>5</sup>Los Alamos National Laboratory, Los Alamos, NM; <sup>6</sup>U.C. San Francisco, San Francisco, CA

<sup>7</sup>The Aerospace Corporation, El Segundo, CA; <sup>8</sup>Utah State University, Logan, UT

<sup>9</sup>The University of New Mexico, Albuquerque, NM

**Abstract.** The imminent return of the Genesis Sample Return Capsule (SRC) from the Earth’s L1 point on September 8, 2004, represents the first opportunity since the Apollo era to study the atmospheric entry of a meter-sized body at or above the Earth’s escape speed. Until now, reentry heating models are based on only one successful reentry with an instrumented vehicle at higher than escape speed, the 22 May 1965 NASA “FIRE 2” experiment. In preparation of an instrumented airborne and ground-based observing campaign, we examined the expected bolide radiation for the reentry of the Genesis SRC. We find that the expected emission spectrum consists mostly of blackbody emission from the SRC surface ( $T \sim 2630$  K @ peak heating), slightly skewed in shape because of a range of surface temperatures. At high enough spectral resolution, shock emission from nitrogen and oxygen atoms, as well as the first positive and first negative bands of  $N_2^+$ , will stand out above this continuum. Carbon atom lines and the 389-nm CN band emission may also be detected, as well as the mid-IR 4.6-micron CO band. The ablation rate can be studied from the signature of trace sodium in the heat shield material, calibrated by the total amount of matter lost from the recovered shield. A pristine collection of the heat shield would also permit the sampling of products of ablation.

Keywords: reentry, fireball, meteor, sample return capsule, Genesis, thermal protection system, astrobiology

### **Introduction**

The *Meteoroids 2004* conference was held at the University of Western Ontario, London, three weeks before the scheduled return of the Sample Return Capsule (SRC) of NASA’s Genesis

---

\* Corresponding author: pjenniskens@mail.arc.nasa.gov

mission on September 08. The return of the Genesis SRC was the first opportunity since the Apollo era to study bodies entering the Earth atmosphere at or above escape speeds. At the meeting, we reported on the process of bringing together an instrumented aircraft campaign (the *Hyperseed Multi-Instrument Aircraft Campaign*) to observe this artificial bolide. We called for further ground-based observations to expand the range of possible measurements.

As part of the preparations for this mission, preflight predictions were performed using the SRC entry trajectory and entry vehicle shape to generate the continuum fluid dynamic flowfield solutions and the expected radiation spectra. This information was used in selecting the instrumentation for remote sensing of the fireball. This report summarizes those predictions.

At the time of writing, the reentry has occurred. Other opportunities will follow (Table I) when the Stardust (Jan. 2006) and Hayabusa (June 2007) SRCs will enter Earth atmosphere (Desai et al., 2000). These fireball observations can help us better understand natural asteroid impacts and can help improve the design of thermal protection materials for future Crew Return Vehicles that will bring people back from the Moon and Mars.

## **Scientific Rationale**

### **1. Sample Return Capsule Entry as an Artificial Meteor.**

Natural impacts of meter-sized asteroids are extremely rare and unannounced, but represent a significant amount of matter falling in on Earth. Their arrival in the atmosphere is heralded by a brilliant flash of light and a burst of sound waves. No observations have been targeted at the specific aspects of ablation and atmospheric chemistry that are important for evaluating the role of meter-sized bodies in the exogenous delivery of organic matter to Earth at the time of the origin of life, for example. Until now, nearly all available data come from staring instruments that are used to "listen" for clandestine nuclear tests and rocket launches and to recover meteorites.

The exogenous delivery of organics by small bodies of the solar system was the topic of past *Leonid Multi-Instrument Aircraft Campaigns*, which targeted the "meteoroids" peak, cometary dust, and the rarefied flow conditions of meteoroids smaller than the mean-free path of air at the altitude of ablation (e.g., Jenniskens et al., 2000a,b). *Hyperseed MAC* will target the meter-sized asteroids, the source of meteorites and rare fireballs, bodies large enough to form a hypersonic shock wave. Meter-sized "boulders" form a second peak in the terrestrial mass influx curve. They could have been the dominant source of organics and water at the time of the origin of life. Water entrapped in primitive asteroids has the D/H ratio of our ocean. Alternative sources of organic matter are giant impacts by asteroids and comets of ~ 10 km in size and ~ 150 micron sized meteoroids, each delivering under different circumstances. Giant impacts created high-pressure, high-temperature, shock waves that destroyed most of the organic matter. Meteoroids, on the other hand, were too small to form shocks, and their organic matter was ablated as a haze of large molecules.

Somewhere in between are the fireballs that result from the impact of meter-sized asteroids. They deposit 99.9% of mass in the Earth's atmosphere in a complex process of ablation, spallation, fragmentation, and shock layer chemistry. The organic matter in the asteroids is deposited in the atmosphere in the form of atoms, small molecules, large molecules, soot, and dust. Carbon atoms and molecules will react chemically with the atmosphere in the shock layer and wake, which could result in organic compounds enriched in functional groups that are different from those found in meteorites.

The tiny fraction that survives in the form of meteorites can be studied in the laboratory. Although meteorites give information on the initial composition of the organic matter and its association with minerals and water, such studies do not address what happens to the bulk of the organic matter in the fireball phase. No samples in our dust collections are with certainty from asteroid entries, although some particles appear to be ablation droplets similar to those found partially attached to the fusion crust of meteorites. Many recovered micrometeorites appear to be of asteroidal origin, but their predominant CM composition suggests they derive from small meteoroids.

We do not know if carbon can survive the shock layer conditions in reduced form as molecules or solid particles. In the present day atmosphere, organic molecules and soot are quickly dispersed and blend with our natural and man-made environment. Laboratory experiments of meteorite ablation mimic, but do not reproduce exactly, the physical conditions in natural fireballs. In particular, it is impossible to reproduce at the same time both the heat flux to the surface from convective flow and from radiation generated just behind the shock.

We understand that the SRC reentries are not natural bolides, but they have similar flow conditions and they provide simpler and well known experimental starting conditions to study various aspects of the ablation process. Their size (0.8 – 1.5 meter) is in the range of asteroid fragments at the peak of mass influx (~ 4 meters). The SRC entry speed (11.0 – 12.9 km/s) is high enough to have a significant contribution from radiative heat flux and sample the lower end of the range for natural asteroid entries (11 to about 30 km/s, peaking around 15 km/s). The Stardust SRC will have the highest heating rate for any Earth returning vehicle to date. The sample return capsules come in at a particular entry angle (~ 8 degrees), creating a nice long duration grazing fireball, while asteroids cover the full range from 0 to 90 degrees. The sample return capsules are blunt objects, setting up a relatively wide shock wave, the size and shape of which affect the heat flux. Asteroids, too, are blunt objects, unlike most sharp re-entering objects studied for military applications. The SRCs are spun up to stabilize the reentry. Natural asteroids spin too, albeit with a spin vector relative to the forward direction of motion that can be different from that of the SRCs. Overall, the conditions in the shock wave are, as far as the processing of the ambient air and heat flow to the surface are concerned, representative of natural bolides. Finally, a big advantage of SRC reentries over natural fireballs is that their emission spectrum is not dominated by metal atom line emissions from the ablated matter. This makes it possible to study the much weaker shock emissions.

An important difference between SRCs and asteroids is that the rate of ablation is low. This will affect the abundance of trace compounds in the ablated layer over the surface. The expected

ablation products along the stagnation streamline at peak heating are dominated by CO, C and C<sub>3</sub> (Olynick et al., 1999). Triatomic carbon, C<sub>3</sub>, and CO mole fractions drop rapidly as the temperature rises in the boundary layer. A similar analysis for Genesis is not published, but we expect the CO mole fractions to be roughly the same but the C<sub>3</sub> and H values to be much lower, depending strongly on the peak surface temperature. Most of the ablation would be due to oxidation, leading to CO and carbon atoms (from the decomposition of CO into C + O away from the surface). Natural asteroids can have lower and higher heat fluxes, depending on entry conditions. They, too, may combust their organic matter incompletely. Such chemistry is of interest to astrobiology. Most of the Genesis carbon-carbon heat shield is ablated over a period of about 40 seconds around peak heating, when the SRC is between 80 and 50 km altitude (bolides ablate between 80 and 20 km).

The asteroids are also prone to catastrophic fragmentation, which leads to much mass being lost in small debris fragments. The sample return capsules are certainly not intended or expected to catastrophically fragment.

**Table I**

	<b>Genesis</b>	<b>Stardust</b>	<b>Hayabusa</b>
Date:	Sept. 08, 2004	Jan 15, 2006	June 2007
Time (local):	9:52:47 a.m. MDT	3:00 a.m. MDT	night time
Elevation Sun:	27°	night time	night time
Moon phase, elevation:	0.7, 72°	1.0 (full), 68°	t.b.d.
Mass (kg):	225	45.8	18
Diameter:	1.52 m Ø	0.811 m Ø	0.40 m Ø
Entry speed (@125 km):	11.0 km/s	12.9 km/s	12.2 km/s
Entry angle:	8.0°	8.0°	12.0°
Attack angle:	2.5 deg.	3.0 deg.	-.-
Spin rate (rpm):	15	15	2
Peak brightness:*	-6.4	-6.7	-5.2
Peak heat rate (W/cm <sup>2</sup> ):	700	1200	~1500
Peak deceleration, Earth g's:	28	34	45
Landing site:	UTTR, Utah	UTTR, Utah	Australia
Heat-shield material:	carbon-carbon	phenolic impregnated carbon	phenolic ablator
Thickness	1.5" over insulator	2"	-.-
Sample returned:	solar wind	comet + I.S. dust	asteroid debris

\*) From 100 km, V-magnitude if blackbody emission only.

## 2. A test of a Thermal Protection System.

The Genesis SRC heat shield material is flown for the first time under these high entry-speed conditions. The actual conditions of descent have never been simulated in the laboratory for all

relevant parameters at the same time. The NASA/Ames Arcjet Facility mimics the convective heat flow well (albeit with pre-dissociated air), while shock-tube experiments provide good measurements of the radiative heat flux (albeit for a brief moment of time). Radiative heat flux becomes important relative to convective heatflux for speeds in excess of  $V > 11$  km/s. This is clearly shown in the models for heat flux of two Apollo missions (Fig. 1). In the case of Genesis, about 5% of the heat flux is expected to be due to radiative heat flux.

Only one successful reentry with a blunt instrumented vehicle at higher than escape speed has been studied in the past. The 22 May 1965 NASA “FIRE 2” experiment consisted of an instrumented subscale model of the Apollo crew return vehicle, boosted to 11.36 km/s. Telemetric data on heat flux were sent to the ground and that data is used even today. No remote observations were made. The Stardust and Genesis thermal protection calculations are based on these FIRE 2 data. The earlier 14 April 1964 NASA “FIRE 1” experiment, boosted to 11.25 km/s, failed because the booster caught up with the model after separation. The lack of data prompted the Japanese space agency JAXA to launch “DASH” – *Demonstrator of Atmospheric Reentry System with Hyper Velocity* on 4 February 2002, boosting to 10.0 km/s a flight model of the Hayabusa SRC (formerly MUSES-C). The experiment failed because SRC and booster did not separate (Maemura, 2002).

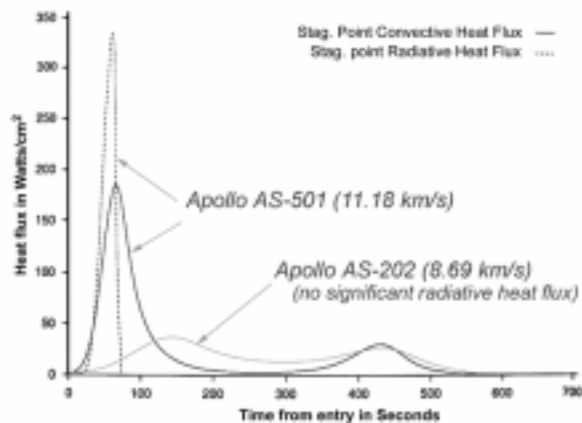


**Fig. 1. Convective (solid line) and Radiative (dashed line) heat flux as a function of time from entry (in seconds) for Apollo returns from Earth orbit (AS-202) and from the Moon (AS-501).**

The FIRE 2 data, and results from Apollo 4, are still being used to calibrate the current NEQAIR models that predict the amount of radiative heating expected. NEQAIR is based on first principles, line-by-line methodology. Emission models are based on spectroscopy data. While that theory is well understood, it is the excitation and transport conditions that are difficult to model and are presently calibrated by few actual entries over a limited range of ablation and entry conditions. Additional flight data over a wide range of entry conditions are needed to provide validation data.

In addition to questions of radiative heating, there are specific issues with the design and materials used in the thermal protection system. If a meteoroid impacted the heat shield prior to entry, the brittle material may have been damaged, as was the carbon-carbon wing edge of the Space Shuttle Columbia (STS-107) during launch. In addition, light can penetrate the SRC carbon fibre structure, heating lower layers, and possibly resulting in spallation. If spallation turns out to be more important than expected, more of the heat shield will be lost.

The surface of the Genesis SRC is a 1.5 inch thermally-conductive high-density ( $1.8 \text{ g/cm}^3$ ) high-temperature (2,870 K) deposited carbon-carbon sheet (made of fibers of highly ordered pyrolytic

carbon) on top of a low density carbon foam insulator. Thus, carbon debris may be created in a manner not typically expected for asteroids. The known properties of the starting material, however, permit testing of the ablation rate as a function of surface temperature against models. Laboratory experiments involving both carbon-carbon and natural meteorite materials can then provide a context to understand the differences in their ablation properties.

The lid of the capsule will pop off at about 36 km altitude, 2.2 minutes after entering Earth’s atmosphere, when a drogue chute is expected to deploy, followed by a parafoil chute almost 4 minutes later at 6.1 km altitude. The parachute will be grabbed with a hook carried by a helicopter before hitting the ground at the Utah Test and Training Range (UTTR) to prevent the sample panels from breaking. This pristine recovery of the heat shield makes it possible to sample carbon flakes and recondensed soot deposits that are products of the ablation.

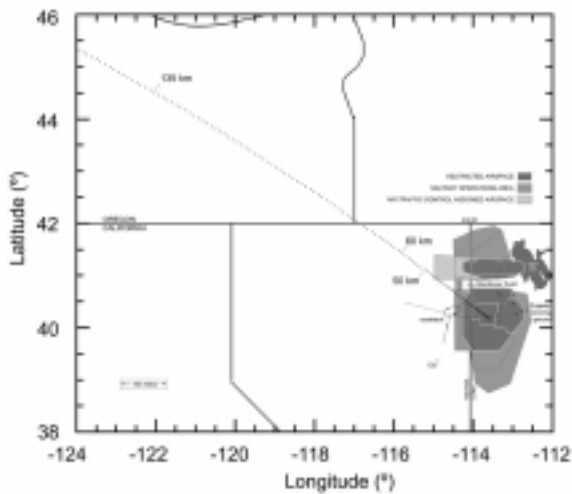


**Fig. 2.** Flight trajectory (intervals in 1 second flight time), with position of the FISTA aircraft (“racetrack”) and location of Utah Test and Training Range.

### Predicted emissions

The Genesis SRC might first be seen at ~100 km altitude (Fig. 2), where the surface temperature starts to rise significantly (Fig. 3). Peak surface temperature, and peak absolute brightness, is at about 60 km altitude and +59 seconds after passing

the 135 km altitude point. Highest deceleration occurs at ~50 km altitude, about 66 s in flight. Once the forward motion has been stopped, the object will fall at a steep angle onto U. T. T. R.. The point of impact is uncertain to many tens of kilometers (Desai and Cheatwood, 1999), but the trajectory is expected to be better known after the Sample Return Capsule has been released from the spacecraft prior to reentry.

Stardust will have a similar approach trajectory coming from the WNW and landing at U. T. T. R.. The higher entry speed is somewhat compensated by its smaller mass, but the peak heating temperature will still be higher. Stardust arrives faster than Genesis and has a Phenolic Impregnated CARbon ablator heatshield (PICA, Tran et al. 1996). Because of that, the peak surface temperature will not rise above 3500 K, at which

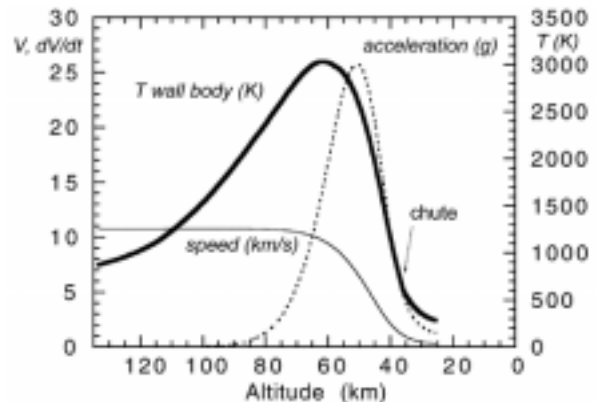


**Fig. 3.** Genesis SRC entry conditions of speed, deceleration, and peak surface temperature versus altitude.

temperature a convective surface layer of compounds (CO, C<sub>3</sub>, air) carries away heat and in effect blocks boundary layer energy from reaching the surface. A similar effect will occur in natural bolides (at lower temperatures), from ablated organic and mineral components. The SRC reentry experiment will provide information on the efficiency of carbon in protecting and cooling the surface in this manner, by simply measuring the surface temperature as a function of altitude and taking into account the measured radiative heat flow derived from the intensity of air plasma emissions (convective heat flow assumed known).

### 1. Blackbody radiation.

If the surface temperature of the SRC rises above about 2500 K, we expect that the blackbody radiation from the surface will dominate the total light output at visible and near-IR wavelengths (Fig. 3). The blackbody radiance is a strong function of surface temperature  $\sim T^4$ .

**Fig. 4.** The wavelength dependent SRC surface blackbody emission for representative temperatures.

The distribution of surface temperatures has a small but significant impact on the expected wavelength dependent signal. Surface temperatures will range from about 2400 to 2923 K, causing light emission to peak near 1 micron. Figure 4 shows the blackbody curve for different temperatures and an “Integrated Surface Intensity” calculated by adding the area-weighted contributions of each surface point.

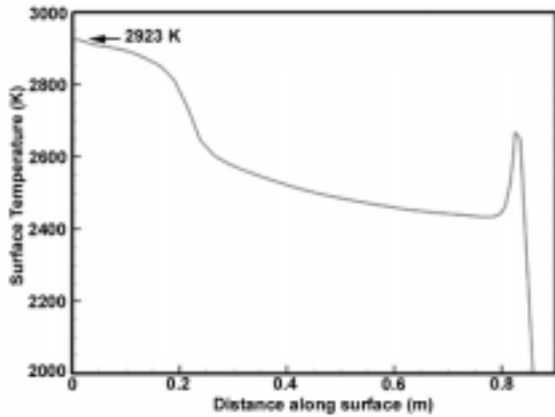
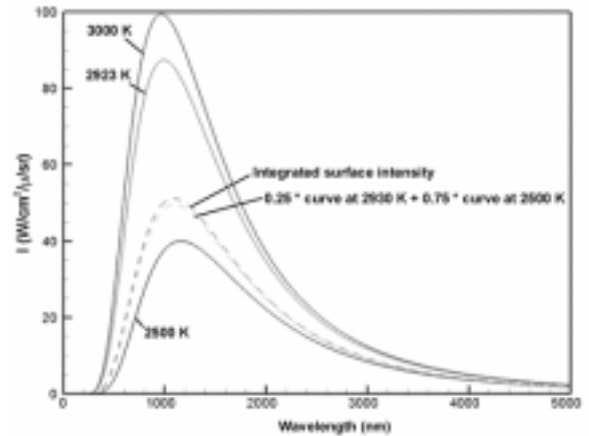


**Fig. 5.** Plot of the radial distribution of the Genesis SRC surface temperatures. A peak temperature of 2923 K is found at time = 126 s for the REF-08 Trajectory. A fully catalytic, radiative equilibrium wall is assumed.

The maximum surface temperature occurs at the stagnation point (Fig. 5), with possible hot spots at the forebody penetration points. These hottest surfaces represent only a small fraction of the total and do not change the shape of the continuum spectrum much. Nevertheless, a small skew may be observed in the blackbody curve, if it can be measured precisely enough over a wide wavelength range.

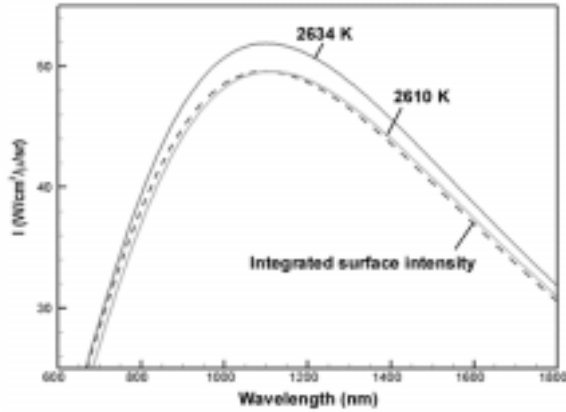


**Fig. 6.** Sum of blackbody emissions (dashed line) from the model shown in Fig. 5, with blackbody curves at  $T = 2610$  and  $T = 2634$  K (solid lines) superposed to see the anomalies.

The observed emission will be characterized by the intermediate temperatures off the stagnation point, with a mean at around 2610 - 2634 K. The integrated distribution would suggest a temperature of  $T \sim 2634$  K at short wavelengths near 700 nm, but  $T \sim 2610$  K

at longer wavelengths near 1600 nm (Fig. 6). These differences may be sufficient to retrieve information about the surface temperature distribution from remote sensing observations. Predicted surface distributions can be compared to the measured intensity distributions to determine the range of possible peak temperatures and distributions.

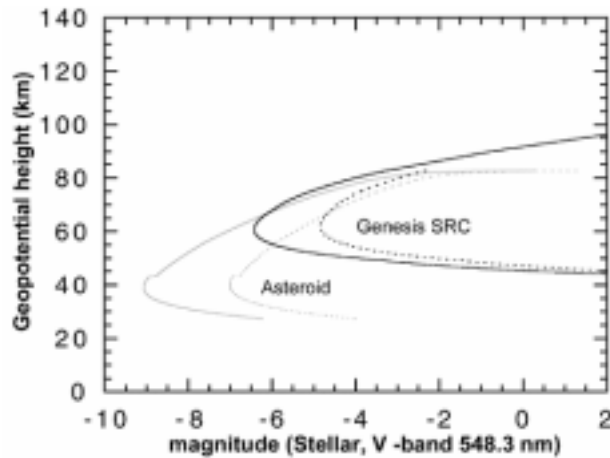


**Fig. 7.** Stellar V magnitude of the SRC in terms of anticipated absolute (= at 100 km distance, solid line) and apparent (from the perspective of FISTA, dashed line) brightness. The result for blackbody emission only (frontal face, black line) is compared to the entry modeling of a natural bolide (gray line), assuming a mass of 225 kg at 11 km/s at an entry angle =  $8^\circ$ .

The blackbody emission alone would make the object bright enough to be detected in broad daylight at visual wavelengths, albeit with some

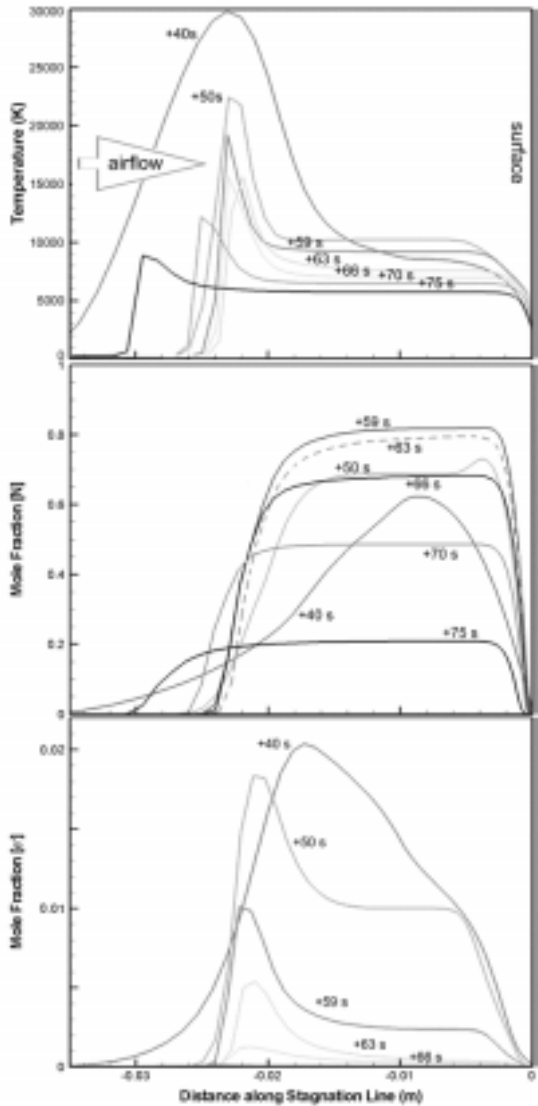
difficulty. Fig. 7 shows the expected SRC brightness based on the blackbody emission alone. The SRC entry was also studied with the more comprehensive asteroid entry bolide model of Doug Revelle (LANL). This model assumes that the light is proportional to the time rate of change of the kinetic energy (through the differential panchromatic luminous efficiency). The result is shown in Fig. 7. The bolide's heating rate is found to peak at about 55 km at a rate very near to the literature estimate for the Genesis SRC:  $1000 \text{ W/cm}^2$ . Nevertheless, its time rate of change is predicted to peak closer to 38 km. This is where the light peaks in the bolide model. The small increase in brightness marks the onset of turbulence in the shock, something that may be observed.

## 2. Shock radiation.

Radiation produced in the high temperature region immediately behind the shock is the cause of radiative heat flux. This radiation is emitted from excited (higher energy) electronic states of atoms/molecules and atomic/molecular interactions with free electrons. Figure 8 shows the physical



conditions and chemical abundances in the shock along the stagnation line. Emission processes are generally well-understood, based on laboratory spectroscopic data and calculations. The rate of produced emission is less certain, because it depends on the excitation conditions and gas density in the shocked layer, as well as the presence of ablation products.



Traditional computational fluid dynamics (CFD) codes compute the number of atoms/molecules in the ground electronic state. An excitation model is needed to calculate the number of electronically excited molecules and the distribution of those molecules among vibrational and rotational states based on CFD results. Models that describe the amount of absorption in the shocked layer are needed to compute the transport of photons from the shock region to the surface and the radiative heating at the surface. The theory for such models is well understood, but the necessary absorption coefficient data is lacking.

**Fig. 8.** Shock conditions at different times during descent. On the X-axis is the distance along the stagnation line (m), on the vertical axis the mole fraction of neutrals and of electrons in the shock layer. The air is impinging from the left, while the surface of the SRC is on the right of the diagrams.

One of us (J.O.) performed CFD (DPLR) calculations for 11 species ( $N_2$ ,  $O_2$ ,  $NO$ ,  $N$ ,  $O$ ,  $N_2^+$ ,  $O_2^+$ ,  $NO^+$ ,  $N^+$ ,  $O^+$ ,  $e^-$ ) at 7 points on the preliminary Genesis trajectory called “REF-08”, which is close to the actual trajectory. Based on the CFD result at each point, NEQAIR calculations were performed over the wavelength range  $0.3 < \lambda < 1.0 \mu m$ . Shorter wavelength measurements are not possible due to atmospheric absorption. Longer wavelength lines and bands are currently not included and/or verified in the NEQAIR model. N and O atomic lines, bound-free & free-free continuum, and  $N_2$ ,  $O_2$ , and  $NO$  molecular bands are included. The shock layer emission in the direction of the observing plane is assumed to be optically thin. We also assume there is no atmospheric absorption between the capsule and the observing plane, which is reasonable. At times prior to  $t = 40$  s, the SRC may not be in the continuum flow regime and the Navier-Stokes results are suspect.

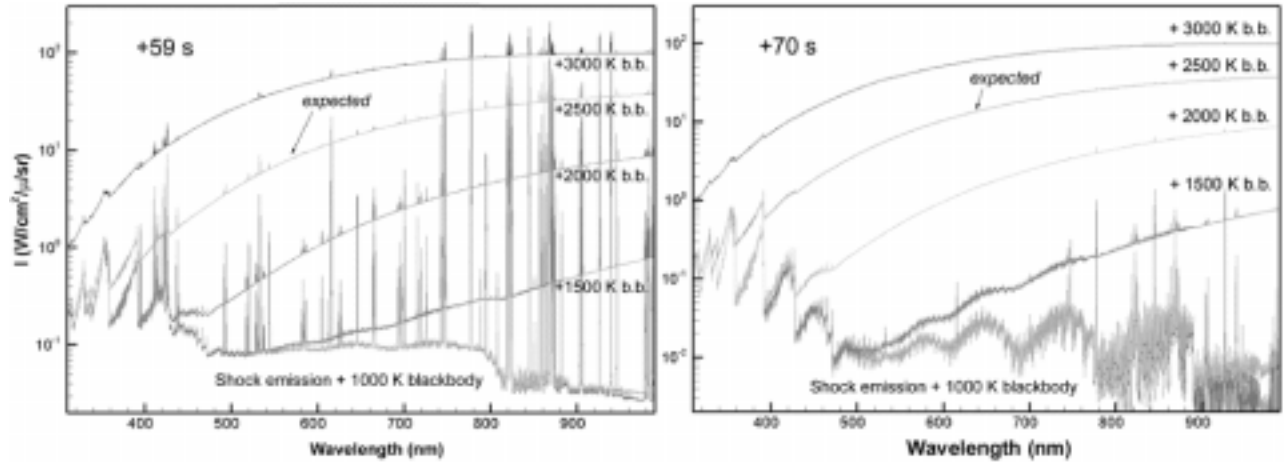


**Fig. 9.** Expected optical emissions from shock radiation (stagnation temperature 2410 K, radiative equilibrium) at  $t = +59$  s (peak heating) and  $t = +70$  s after entry, superimposed on various blackbody radiation levels.

Fig. 9 shows the sum of shock emissions and surface blackbody radiation during peak heating. The excitation temperatures in the shock vary, but the primary radiators include the  $N_2[1^+]$  band, the  $N_2^+[1^+]$  band, and N and O lines. There is also a weak continuum from the air plasma. The shock radiation is primarily emitted from the “overshoot” region immediately behind the shock wave and is stronger in the early phases of heating. The adopted radiative equilibrium stagnation point temperature ( $T = 2410$  K) is an upper bound on the temperature. The blackbody curves represent the integrated average surface temperatures expected at different times during descent. The shock layer emission shown represents a volume-averaged value.

We find that band emission below 400 nm and the near-IR atomic lines of oxygen and nitrogen should be discernible even early in the trajectory. At a spectral resolution of 1 nm, band emission below 450 nm and atomic lines should be discernible at peak heating. Band emission below 400 nm and atomic lines should be discernible past peak pressure, when both shock emissions and surface emissions are weaker. A higher spectral resolution will cause the atomic lines to stand out better from the blackbody background.

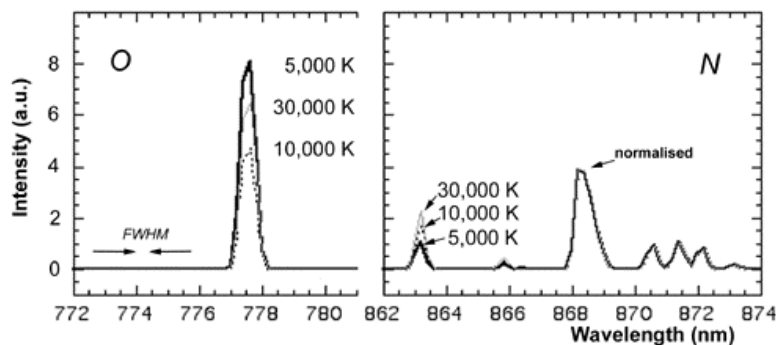
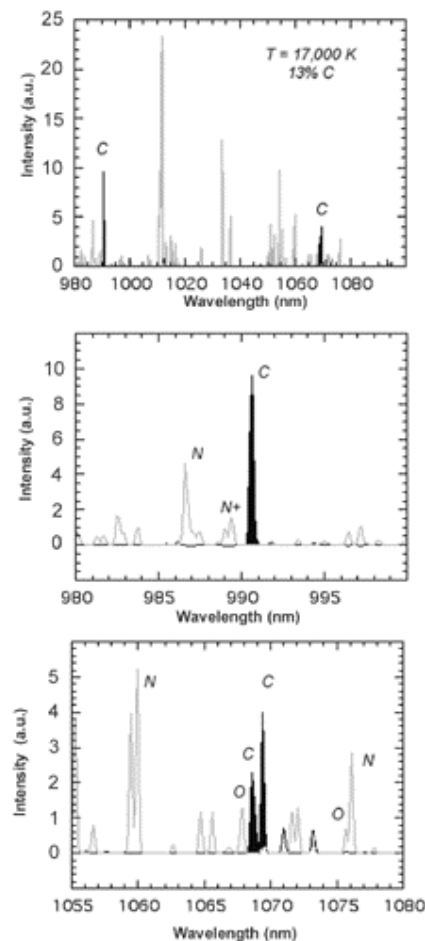


**Fig. 10.** The various nitrogen and oxygen lines at 0.34 nm resolution for different excitation temperatures (in K).

The line ratios among nitrogen and oxygen lines (Fig. 10) are useful thermometers of excitation temperatures (for a given species)

and chemical abundances in the air plasma (ratio of  $N/N^+$  versus  $O/O^+$ ). The absolute line intensities provide deviations from Local Thermodynamic Equilibrium. The optical and near-IR emissions are proportional to the far UV emissions at  $\sim 120$  nm that can not be seen from the ground or air, but which are important for radiative heating. The air plasma emissions need to be resolved from the blackbody background continuum at sufficient signal to noise to measure line intensity ratios precisely enough.



### 3. Emissions from ablation products.

We did not yet consider the effect of surface blowing and ablation products (CN, CO, C,  $C_2$ , etc.). Preliminary calculations of ablation products show that the CN Violet band around 400 nm may be detectable, even though abundances are expected to be low (Olynick et al., 1999). CN is generated from the interaction of carbon atoms from the surface with the nitrogen in the shock layer. The emission may be more intense for the Stardust reentry, which is expected to ablate significant amounts of carbon in the form of atoms and  $C_3$ . At mid-IR wavelengths, the 4.7-micron CO band should be detectable if detected on top of a well defined blackbody slope. The emission is expected to be broad. The Stardust heat shield will also generate significant amounts of C, and  $C_3$ .  $C_3$  has a broad emission band just above the mid-IR CO band.

**Fig. 11.** The possible intensity of carbon atom lines in relation to N and O lines for an excitation temperature of  $T = 17,000$  K.

In the process of making the carbon-carbon material, a binding component containing sodium left traces in the fibers. We propose to measure ablation rate from the sodium D-line intensity, even when the rate is low. Sodium is an atom with a zero energy ground state and high transition probability, but is also expected to rapidly ionize in the shock layer after leaving the surface. Hence, the intensity of the sodium emissions are expected to be proportional to the rate of ablation. Because of that, the sodium emission can serve as a tracer of the ablation profile. The ablation rate can be calibrated from the total amount of material lost from the recovered heat shield. Atmospheric trace sodium found between 90 and 80 km does not contribute significantly to the spectrum, as is demonstrated by sodium-deficient meteor spectra.

The forebody penetrations, too, may cause strong metal atom line emissions, but from the metals that underlay the carbon-carbon heat shield, which include aluminum and titanium. We also recognize a small probability of heat shield spallation, which can lead to small fragments being lost. Those could be seen as points of light quickly trailing the capsule due to higher surface-to-mass ratio and rapid deceleration.

A much more difficult target is the carbon atom line emission. The strongest accessible lines of atomic carbon in ground or airborne observations are in the near-IR at 966, 991, and 1069 nm. Thirty-four seconds in flight, the flux of ablated material is 13% of the amount of impinging air, the highest ratio. The ablated materials penetrate deeper into the shock layer early on in the trajectory. From that, the expected emission spectrum (Fig. 11) has carbon lines nearly as strong as nitrogen and oxygen lines in the 900 - 1100 nm wavelength region. To avoid blending and to bring out the lines from the strong continuum, a high spectral resolution  $< 1$  nm is needed. Shown are data at 0.25 nm resolution.

Mid-IR measurements of CO (4.67 micron), and C<sub>3</sub> (5.2 micron) emission in the case of Stardust, would not only provide a measure of abundance of ablated compounds, but also the temperature of the emitting molecules from the band shape (expected to be anywhere from  $\sim 3,500 - 10,000$  K). The ratio of CO and C<sub>3</sub> band strengths is a sensitive indicator of the relative importance of oxidation and sublimation under the given conditions. The observations would need to be capable of measuring the band strengths above the (relatively weak, peak at shorter wavelength) continuum, taking into account a possible variable water vapor absorption band above 5.3 micron. Above 1,000 K, the 4.67 micron CO band has a distinct band head at 4.3 micron, a peak at 4.5 micron, and the band stretching to longer wavelengths out to 5.5 micron (Russell et al. 2000). Although the band head falls in the telluric CO<sub>2</sub> absorption, the attenuated emission can be recognised because the CO band falls off steeply, by a factor of 40, from 4.67 to 4.0 micron. Hence, it is important to measure the continuum in the 3.5 – 4.0 micron region to measure the CO band strength reliably. With a peak ablation rate of 0.5 kg/s for Genesis (and 0.2 kg/s for Stardust), nearly all of which goes into CO and, using that optically thin CO at 3500 K emits at a rate of 3 photons/sr/micron/molecule at the instrument resolution (Russell et al., 2000), the CO band intensity would be 145 % of the continuum emission at the peak of ablation.

The expected emissions of hot complex carbon molecules, clusters, flakes, and soot grains  $< 10$  microns in size have peaks at 6.2 and 7.7 micron due to C-C stretch and bend vibrations. Reactions with atmospheric water and hydrogen can result in a C-H emission band at 3.4 micron, as will the Stardust phenolic impregnated carbon. Little is known about the expected amounts of these materials, which can be deduced from excess emission in the 6-8 micron range.

#### **4. Other interesting phenomena.**

Any wake emissions are thought to be dominated by NO<sub>2</sub> chemiluminescence in the visible. This is a broadband emission hard to distinguish from continuum.

The strong hypersonic shock wave is expected to generate an infrasound signal on the ground. The predicted peak-to-peak amplitude pressure difference is 1-5 Pa, derived from Apollo entry data from various NASA reports, scaled to the much smaller size of the Genesis SRC.

Worth investigating is also the possible existence of a large photoionization halo generated by "precursor" UV radiation from the shock wave. Radio echoes have been detected before from a manned space vehicle returning to Earth (Lin 1962) and attributed to this effect. The UV-precursor mechanism had been invoked earlier to explain meteor head echoes (Cook and Hawkins 1960). The effect has been demonstrated, for near continuum flows, in laboratory shock tube experiments (Presley and Omura 1970). The ionizing radiation is believed to be from electronic states in  $N_2$  sufficiently energetic to ionize  $O_2$  (Marrone and Wurster 1970).



*Fig. 12. Hyperseed MAC Genesis team at Edwards AFB, California (Sept. 03, 2004). Photo: USAF/412<sup>th</sup> TW.*

## **Hyperseed MAC**

Motivated by this rare scientific opportunity, we have worked to provide an airborne platform for a diverse team of researchers. The USAF/412<sup>th</sup> TW operated "FISTA" aircraft, an NKC-135, and the same aircraft used in past Leonid MAC missions (Jenniskens et al. 2000b), has 20 upward looking windows of 12" inch diameter optical quality glass. USAF Hanscom AFB will provide the optical windows, including one of Germanium for mid-IR observations. The aircraft permits viewing of the SRC above weather, water vapor, smoke of wild fire and other aerosols, providing a low sky background in the visual and near-UV, and low scintillation for imaging. The SETI Institute will provide the logistic support.

Participants (Fig. 12) will be from NASA Ames Research Center, the SETI Institute, the Aerospace Corporation, the University of Alaska, the USAF Academy, Utah State University, the University of New Mexico, Los Alamos National Laboratory, Sandia National Laboratory, Lockheed Martin, and U.C. San Francisco. An overview of instrumental capabilities is given in Fig. 13. Spectroscopic instruments will be mostly slit-less, but we will also include a tracking device ("AIMIT") with a high-resolution slit-spectrograph to resolve atomic line emissions. Some redundancy will be provided. Optical and near-UV spectrometers will focus on the CN and  $N_2^+$  emission bands, and the sodium and N & O atomic lines in the red and near-IR. Near-IR (InGaAs) spectrometers will measure the peak of the blackbody curve and any broadband molecular emissions in the range 900-1600 nm. Mid-IR sensors will study the blackbody emission tail and any CO and CO<sub>2</sub> vibration band emissions. High frame-rate imagers and photometers will observe any irregularities in light output, spallation, and the development of a UV halo. Telescopic systems are also included to attempt to obtain spatial features of SRC, but we do not expect to resolve features above  $\sim 10$  meters. These instruments will be hand-pointed, using pointing cameras with  $\sim 5 - 10^\circ$  field of view, small enough to bring out the SRC from the bright daytime background. The nighttime reentry of Stardust will not require such restrictions.

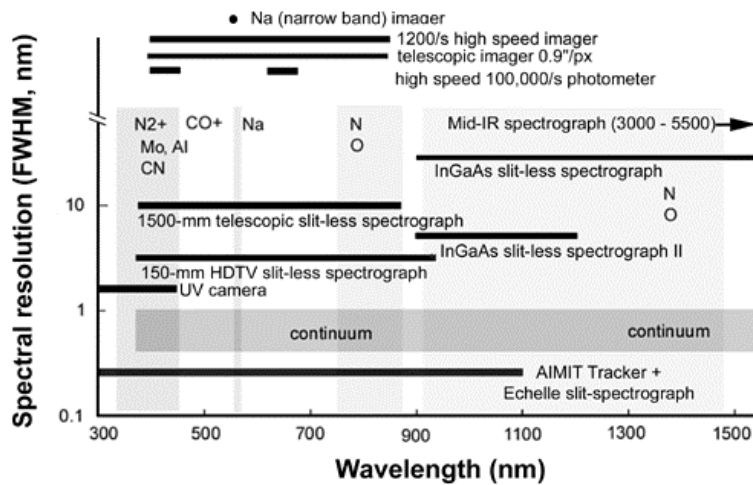


**Fig. 13.** Outline of instrumental capabilities.

Different instruments will cover different dynamical ranges in brightness and different spectral resolutions. Photometry will tie the various spectral ranges together (allowing for different beam filling factors and some redundancy).

This will be a one-day mission out of Edwards AFB in southern California to Oregon (~ 2 hour flight), where the

aircraft will be positioned along the track of the approaching reentry vehicle so that the object has the lowest angular velocity upon approach (Figure 2). This permits observing the shock from the front, but also have a gradual increasing apparent motion on the sky to be able to study any wake. Because the measurements will be done from one location, the results from different instruments can be compared.

The airborne observations will be complimented, however, with a number of ground-based observations. In particular, an infrasound array will be installed at Wendover Airfield, Nevada (Figure 2). The array is composed of four, low-frequency pressure sensors with spatial wind-noise filters with a horizontal separation of ~50-100 m between individual sensors. The basic pressure sensor is a Chaparral microphone with flat response (3 dB band-pass) from 0.02 to 10 Hz for signal amplitudes as small as 0.01 Pa.

## Conclusions

Preflight predictions performed using SRC entry trajectory, entry vehicle shape to generate CFD flowfield solutions, and theoretical radiation spectra show that blackbody radiation is expected to dominate the emissions, but there will also be significant shock emissions and emissions from ablated compounds. An instrument suite was selected which is expected to provide appropriate sensitivity to wavelength and intensity of important features.

The mission will aim to confirm the average surface temperature and temperature profile due to the combined radiative and convective heat flux. We will attempt to measure the intensity of the shock emissions to estimate the contribution from radiative heat flux and perhaps detect the transition to turbulent flow. Detection of shock emission will also permit the study of the physical conditions for shock chemistry in natural bolides.

The ablation profile appears to be most readily studied from the expected sodium emissions, assuming that the sodium intensity is proportional to the number of atoms released per second into the shock. The possible detection of CO in the mid-IR can confirm that burning towards CO is the dominant ablation process. Imaging of any wake and sparks can confirm whether or not spallation occurred during descent.

These observations may assist in an accident investigation in the (remote) case of catastrophic failure during descent. Of particular interest in this regard is damage in space and the impact of the forebody penetrations on the ablation behavior of the heat shield.

*Final note.* At the time of writing, the Genesis SRC entry is behind us. The heat shield performed much as expected, but due to a technical design error, the drogue chute did not open. The Hyperseed MAC mission was executed much as planned. The observed entry trajectory was very close to that predicted hours before the reentry. Unfortunately, all narrow-field pointed instruments failed to acquire the SRC because an outdated trajectory file was used by mistake to calculate the pointing directions. Direct access to the latest predicted trajectories from the primary mission navigator source can help prevent this mistake in future missions. We did successfully acquire the SRC with staring broadband imagers from the plane and ground, providing surface temperature measurements, and also measured the sonic boom with the infrasound array. These data are still being reduced and the preliminary results were submitted to the accident investigation board.

*Acknowledgments* – Preparations for the Hyperseed MAC mission were supported by NASA Ames Research Center, the Aerospace Corporation, Los Alamos National Laboratory, Sandia National Laboratory, and the SETI Institute. Special thanks go to Maj. John Haser, Don Bustillos, and the staff of the USAF/412<sup>th</sup> TW for support of the FISTA operations. At NASA Ames, management support was provided by Chuck Smith, Guenter Riegler, and center director Scott Hubbard. Our public outreach effort met with educational goals of NASA and the Pro-Amat working group of IAU Commission 22. The Hyperseed MAC mission was financially supported by a grant from the NASA Engineering Safety Council.

*Editorial handling:*

## References

- Cook, A.F., and Hawkins, G.S., 1960. The meteoric head echo. *Smiths. Contr. to Astrophys.* **5**, 1-7.
- Desai, P. N., Mitcheltree, R. A., and Cheatwood, F. M., 2000. Sample return missions in the coming decade. 51<sup>st</sup> International Astronautical Conference, 2-6 Oct. 2000, Rio de Janeiro, Brazil, IAF-00-Q.2.04.
- Desai, P. N., and Cheatwood F. M., 1999. Entry dispersion analysis of the Genesis Sample Return Capsule. AAS/AIAA Astrodynamics Specialist Conference, Girdwood, Alaska, AAS Paper No. 99-469.

- Jenniskens, P., Wilson, M. A., Packan, D., Laux, C. O., Krueger, C. H., Boyd, I. D., Popova, O. P., and Fonda, M., 2000a. Meteors: A delivery mechanism of organic matter to the early Earth. *Earth, Moon and Planets* **82-83**, 57-70.
- Jenniskens, P., Butow, S. J., and Fonda, M., 2000b. The 1999 Leonid Multi-Instrument Aircraft Campaign - an early review. *Earth, Moon and Planets* **82-83**, 1-26.
- Lin S.-C., 1962. Radio echoes from a manned satellite during re-entry. *J. Geophys. Res.* **67**, 1962, 3851-3869.
- Maemura, T., 2002. H-2A Launch vehicle test flight results and the plan for the future. 34<sup>th</sup> COSPAR Scientific Assembly, Houston, Texas, p. V-1-12 (abstract); NASDA Report No. 117, 2002. Headlines. NASDA Public Affairs Office, internal publication.
- Marrone, P. V., and Wurster, W. H., 1970. Reentry precursor plasma – determination of the vacuum ultraviolet photoionizing radiation flux, *The Entry Plasma Sheath and its Effects on Space Vehicle Electromagnetic Systems*, Vol. 1. NASA SP-252.
- Olynick D., Chen, Y.-K., and Tauber, M. E., 1999. Aerothermodynamics of the Stardust Sample Return Capsule. *J. Spacecraft and Rockets* **36**, 422-462.
- Presley, L. R., and Omura, M., 1970. Microwave measurement of precursor electron densities ahead of shock waves in air at velocities greater than 10 km/s”, AIAA Paper 70-83.
- Russell, R. W., Rossano, G. S., Chatelain, M. A., Lynch, D. K., Tessensohn, T. K., Abendroth, E., Kim, D., and Jenniskens, P., 2000. Mid-Infrared spectroscopy of persistent Leonid trains. *Earth, Moon and Planets* **82-83**, 439-456.
- Tran, H., Johnson, C., Rasky, D., Hui, F., Chen, Y. K., and Hus, M., 1996. Phenolic impregnated carbon ablators (PICA) for Discovery Class missions. AIAA Paper No. 96-1911.